

Update on the improved lattice calculation of direct CP-violation in K decays

Christopher Kelly^{*†}

Columbia University

E-mail: ckelly@phys.columbia.edu

Tianle Wang

Columbia University

E-mail: tw2507@columbia.edu

We provide an update on the RBC & UKQCD lattice calculation of the measure of Standard Model direct CP-violation in kaon decays, ϵ'

The 36th Annual International Symposium on Lattice Field Theory - LATTICE2018

22-28 July, 2018

Michigan State University, East Lansing, Michigan, USA.

^{*}Speaker.

[†]This calculation was carried out under the INCITE Program of the US DOE on the IBM Blue Gene/Q (BG/Q) Mira machine at the Argonne Leadership Class Facility, a DOE Office of Science Facility supported under Contract De-AC02-06CH11357; on the STFC-funded “DiRAC” BG/Q system in the Advanced Computing Facility at the University of Edinburgh; on the BG/Q computers of the RIKEN BNL Research Center and the Brookhaven National Laboratory; on the Cori system of the National Energy Research Scientific Computing Center (NERSC), a DOE Office of Science User Facility operated under Contract No. DE-AC02-05CH11231; and on the HOKUSAI “BigWaterfall” machine managed by the RIKEN Advanced Center for Computing and Communications. The DiRAC equipment was funded by BIS National e-infrastructure capital grants ST/K000411/1, STFC capital grant ST/H008845/1, and STFC DiRAC Operations grants ST/K005804/1 and ST/K005790/1. DiRAC is part of the National e-Infrastructure. C.K is supported by the Intel Corporation. T.W. is partially supported by US DOE grant #DE-SC0011941.

1. Introduction

Direct CP-violation – the violation of CP in particle decays – requires the participation of all three quark flavor doublets and is therefore highly suppressed in the Standard Model. As such it offers a promising avenue in which to search for new physics that might help to explain the apparent insufficiency of Standard Model CP-violation (CPV) to account for the matter/antimatter asymmetry in the Universe. This type of CPV was first observed in the decay of neutral kaons into two pions during the late 1990s at the NA31/NA48 experiments at CERN and the KTeV experiment at FermiLab, for which the following value was obtained:

$$\text{Re}(\varepsilon'/\varepsilon) \approx \frac{1}{6} \left(1 - \left| \frac{\eta_{00}}{\eta_{\pm}} \right|^2 \right) = 16.6(2.3) \times 10^{-4}, \quad (1.1)$$

where ε' and ε are the measures of direct and indirect CPV, respectively, and $\eta_{ij} = A(K_L \rightarrow \pi_i \pi_j)/A(K_S \rightarrow \pi_i \pi_j)$. Unfortunately this quantity receives large non-perturbative QCD corrections and therefore it is only recently that a reliable Standard Model prediction has become possible.

In 2015 the RBC & UKQCD collaborations published [1] the first direct calculation of ε' in the Standard Model using lattice QCD via the isospin-definite amplitudes $A_I = K \rightarrow (\pi\pi)_I$, where I refers to the isospin of the $\pi\pi$ state. These amplitudes are computed as

$$A_I = F \frac{G_F}{\sqrt{2}} V_{us}^* V_{ud} [z_i(\mu) + \tau y_i(\mu)] Z_{ij}(\mu) \langle (\pi\pi)_I | Q_j(\mu) | K \rangle, \quad (1.2)$$

where F is the Lellouch-Lüscher factor [2] that represents the finite-volume correction to the decay amplitude, z and y are c-number Wilson coefficients [3], $\tau = -V_{ts}^* V_{td}/V_{ud} V_{us}^*$, V_{ij} are CKM matrix elements, and Q_j are a set of dimension-six four-quark operators. Z_{ij} is the renormalization matrix relating the bare lattice operators to $\overline{\text{MS}}$ operators normalized at the scale μ , thereby matching the scheme used in the calculation of the Wilson coefficients. We obtained the following result:

$$\begin{aligned} \text{Re} \left(\frac{\varepsilon'}{\varepsilon} \right) &= \text{Re} \left\{ \frac{i\omega e^{i(\delta_2 - \delta_0)}}{\sqrt{2}\varepsilon} \left[\frac{\text{Im}A_2}{\text{Re}A_2} - \frac{\text{Im}A_0}{\text{Re}A_0} \right] \right\} \\ &= 1.38(5.15)(4.59) \times 10^{-4}, \end{aligned} \quad (1.3)$$

where the errors are statistical and systematic, respectively. Here δ_l are the s-wave $\pi\pi$ -scattering phase shifts and $\omega = \text{Re}A_2/\text{Re}A_0$.

While the total error on this calculation is roughly three times the experimental error, it is clear that ε' is now a quantity that is accessible to lattice QCD, and our focus since that time has been to improve our statistical errors and our understanding of the systematic errors. In this document we provide an update on the status of this improved calculation.

2. $I = 0$ $\pi\pi$ phase-shift puzzle

The calculation of A_0 requires the determination of the finite-volume $I = 0$ $\pi\pi$ energy. Through the use of G-parity boundary conditions, which increase the ground-state pion momentum from 0 to π/L where L is the lattice box size, this energy is approximately equal to that of the kaon

thus ensuring a physical decay. We compute this from the large-time dependence of the two-point function of an operator that projects onto the $I = 0$ $\pi\pi$ state. We obtain such an operator by combining pion creation/annihilation operators separated by 4 timeslices with back-to-back momenta in the set $(\pm 1, \pm 1, \pm 1)\frac{\pi}{L}$. The average of these eight $\pi\pi$ operators projects onto the A_1 representation of the cubic group. We refer to this averaged operator by the label $\mathcal{O}_{\pi\pi(111)}$.

From the ground-state energy we infer the $I = 0$ s-wave $\pi\pi$ scattering phase shift at the kaon energy scale via the Lüscher formalism [4], for which we obtained $\delta_0 = 23.8(4.9)(1.2)^\circ$ [1]. This number is a few ($\sim 2\sigma$) standard deviations smaller than the value of $\sim 34^\circ$ obtained by combining dispersion theory with experimental input [5]. Here we quote only an approximate value as the dispersive calculation gives the phase shift as a function of the $\pi\pi$ energy, hence any systematic error on the lattice determination will feed into the scale at which the comparison is performed.

Since the 2015 result we have increased our statistics from 216 configurations to over 1400. At this conference we presented [6] a preliminary analysis of the $\pi\pi$ energy with this expanded data set, demonstrating this inconsistency has increased to over 5σ .

A possible explanation for this discrepancy is contamination from a nearby excited state, although there remains no evidence of this from multi-exponential fits to our single-operator ($\mathcal{O}_{\pi\pi(111)}$) correlation functions despite the substantial increase in statistics. A finite-volume state with a nearby energy of ~ 770 MeV is however predicted by combining Lüscher's formalism with phase shifts obtained from dispersion theory. In order to account for this possibility we last year reported [7] the addition of a second, scalar $\pi\pi$ operator \mathcal{O}_σ to our two-point function calculation. In Ref. [6] we also present a preliminary combined analysis of \mathcal{O}_σ and $\mathcal{O}_{\pi\pi(111)}$ two-point functions on 830 configurations, in which we find strong evidence of a nearby excited state and obtain a value for the ground-state phase shift of $\delta_0 = 30.9(1.5)(3.0)^\circ$ that is now compatible with the dispersive result. The effects of adding this operator are illustrated in Fig. 1.

We are presently investigating the effect of this excited state on our calculation of ε' . Since the two-operator data was collected only for the $\pi\pi$ scattering amplitudes, we cannot immediately use the second operator to improve this calculation. In the following section we discuss our efforts to address this issue.

3. Expansion of the calculation of A_0

In response to our observation of a nearby excited state in the $\pi\pi$ system, we recently began computation of $K \rightarrow \pi\pi$ matrix elements with the \mathcal{O}_σ operator. This is a non-trivial extension of our calculation as it involves linear combinations of over 100 Wick contractions that must be carefully derived and implemented/optimized in our high performance lattice simulation environment.

We have also added a third $\pi\pi$ operator to both the two-point and three-point functions, comprising two single-pion operators with back-to-back momenta in the set $(\pm 3, \pm 1, \pm 1)\frac{\pi}{L}$ and permutations thereof. The average of these 24 operators again projects onto the A_1 representation of the cubic group, and we refer to this operator as $\mathcal{O}_{\pi\pi(311)}$.

In addition we have also begun computing $\pi\pi$ two-point functions with non-zero total momentum. In our all-to-all propagator environment [8] these are obtained simply by combining in a different order the ‘‘meson fields’’ computed for the stationary $\pi\pi$ correlation functions. This will yield measurements of the phase shift at a range of lower center-of-mass energies, providing further data that can be compared to the dispersive calculation and also enabling a first-principles lat-

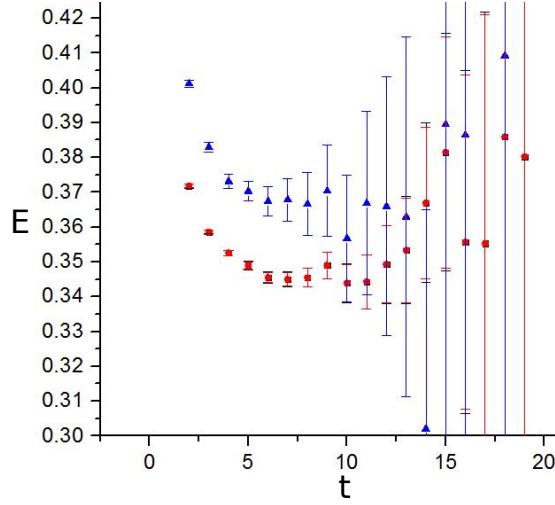


Figure 1: An illustration of the effect of adding the second $\pi\pi$ operator. The upper (blue) curve is the two-point effective mass with just the $\mathcal{O}_{\pi\pi(111)}$ operator. The lower (red) curve is the result of projecting onto the ground-state by taking linear combinations of $\mathcal{O}_{\pi\pi(111)}$ and \mathcal{O}_{σ} with coefficients determined from our fits. We see that the lower curve plateaus at a significantly lower energy, suggesting that the upper curve contains substantial excited state contamination and that a lower large-time ground-state plateau (consistent with the red points) is lost in the noise.

tice calculation of the energy-derivative of the phase-shift, which enters into the Lellouch-Lüscher finite-volume correction to A_0 and that currently accounts for an 11% systematic error on our calculation. We intend to publish a dedicated study of these phase-shifts in the near future.

In order to make this significantly-expanded calculation computationally tractable it was necessary to perform a number of optimizations, which we detail in the following section.

4. Optimizing the expanded calculation

On 512-nodes of IBM BlueGene/Q (BG/Q) computer the $\pi\pi$ two point function contractions with the $\mathcal{O}_{\pi\pi(111)}$ operator require 13.6 minutes for the $8 \times 8 = 64$ different source/sink momentum combinations. In the expanded calculation we include the $\mathcal{O}_{\pi\pi(311)}$ operator and compute correlation functions with $\pi\pi$ total momenta of $(0, 0, 0)$, $(\pm 1, 0, 0) \frac{2\pi}{L}$, $(\pm 1, \pm 1, 0) \frac{2\pi}{L}$ and $(\pm 1, \pm 1, \pm 1) \frac{2\pi}{L}$. This increases the number of momentum combinations to 7848 and would require 27.8 hours to perform just this small aspect of the calculation. In order to make this tractable we investigated the effect of taking advantage of several lattice symmetries in order to reduce the number of contractions needed. The goal was to determine symmetries that could be used without degrading the statistical precision of the calculation. This study was performed using 1438 configurations of two-point data with the $\mathcal{O}_{\pi\pi(111)}$ operator and zero total momentum, and also 121 configurations of data with non-zero total momentum. We considered three different symmetries: parity, i.e. replacing \vec{p} with $-\vec{p}$; the axis permutation symmetry whereby momentum components are globally interchanged; and the “auxiliary-diagram” symmetry that we describe below.

Consider the Wick contraction in Figure 2, where we have labeled the vertices anticlockwise with coordinates $A - D$ that represent both the time and momentum, i.e. $A = (t_A, \vec{p}_A)$. We have

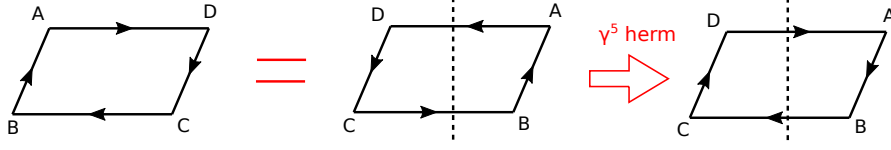


Figure 2: The “direct” and “round-the-world” contraction in which the sink connects to the image of the source in the lattice time boundary (dashed line), both contribute to the measured lattice $\pi\pi$ two-point function, thus measuring these diagrams as if they were independent would yield the same result. The γ^5 -hermiticity of the propagators results in both contributions having the same form.

| Quantity | Orig (64) | Pty+perm (10) | Aux+pty+perm (8) |
|------------------|------------|---------------|------------------|
| $ A_{\pi\pi} ^2$ | 0.1609(22) | 0.1615(24) | 0.1601(24) |
| $E_{\pi\pi}$ | 0.3686(33) | 0.3690(36) | 0.3672(36) |

Table 1: Fit results to the zero total momentum $\pi\pi$ two-point function using 1438 configurations and the $\mathcal{O}_{\pi\pi(111)}$ operator. In the second column we give the result obtained from the full set of $8^2 = 64$ source/sink momentum combinations; in the third we use the parity and axis permutation symmetries to reduce the number of momentum combinations to 10, and in the final column we add the auxiliary diagram symmetry reducing this further to just 8 combinations. The number of combinations in each case is given in parentheses.

$\vec{p}_A + \vec{p}_B = -(\vec{p}_C + \vec{p}_D) = \vec{p}_{\text{tot}}$ where \vec{p}_{tot} is the total momentum, and $t_A - t_B = t_D - t_C = \Delta$ where $\Delta = 4$ is the separation of the two individual pion operators in two-pion operator. As the lattice calculation is performed in a finite box with antiperiodic quark boundary conditions, it is equally valid to consider the measured correlation function as either the direct contraction of the source and sink $\pi\pi$ operators or the “round-the-world” contraction of the sink operator with the image of the source operator in the boundary. Due to γ^5 hermiticity both contractions have the same functional form C as indicated in the figure. Giving the coordinates in anticlockwise order this implies

$$C(A, B, C, D) \equiv C(D, C, B + L_T \hat{t}, A + L_T \hat{t}) \quad (4.1)$$

where \hat{t} is a unit vector in the time direction. Utilizing the time translation symmetry we translate the lhs. by $-t_A$ and the rhs. by $-t_D = -t_C - \Delta$. With explicit coordinates this gives

$$C\left((0, \vec{p}_A), (L_T - \Delta, \vec{p}_B), (\tau, \vec{p}_C), (\tau + \Delta, \vec{p}_D)\right) \equiv C\left((0, \vec{p}_D), (L_T - \Delta, \vec{p}_C), (L_T - \tau - 2\Delta, \vec{p}_B), (L_T - \tau - \Delta, \vec{p}_A)\right) \\ \equiv C\left((0, \vec{p}_D), (L_T - \Delta, \vec{p}_C), (\tau, \vec{p}_B), (\tau + \Delta, \vec{p}_A)\right),$$

where $\tau = t_C - t_A$ and on the second line we have used the reflection symmetry of the correlator under $\tau \rightarrow L_T - \tau - 2\Delta$. A similar relation is found for the other Wick contraction topologies. Writing the full $\pi\pi$ correlator in terms of τ , \vec{p}_{tot} and the *inner* pion momenta of the lhs., $\vec{p}_{\pi_1^{\text{src}}} \equiv \vec{p}_A$ and $\vec{p}_{\pi_1^{\text{snk}}} \equiv \vec{p}_C$; the “auxiliary diagram symmetry” is as follows:

$$C_{\pi\pi}(\tau; \vec{p}_{\pi_1^{\text{src}}}, \vec{p}_{\pi_1^{\text{snk}}}, \vec{p}_{\text{tot}}) \equiv C_{\pi\pi}(\tau; -\vec{p}_{\text{tot}} - \vec{p}_{\pi_1^{\text{snk}}}, \vec{p}_{\text{tot}} - \vec{p}_{\pi_1^{\text{src}}}, -\vec{p}_{\text{tot}}). \quad (4.2)$$

In Table 1 we demonstrate that applying these symmetries in the case of zero total $\pi\pi$ momentum reduces the number of source/sink momentum combinations required from 64 to just 8 without any significant effect on the statistical error. For the moving $\pi\pi$ measurements we show in

| Quantity | Orig (96) | Pty (48) | Pty+perm (16) | Fix \vec{p}_{tot} (Pty+aux+perm) (21) |
|------------------|------------|------------|---------------|--|
| $ A_{\pi\pi} ^2$ | 0.3466(41) | 0.3462(42) | 0.3478(64) | 0.3464(41) |
| $E_{\pi\pi}$ | 0.3869(23) | 0.3869(23) | 0.3879(40) | 0.3868(23) |

Table 2: Fit results to the $\pi\pi$ two-point function with total momentum $(\pm 1, 0, 0)\frac{2\pi}{L}$ (+permutations) using 121 configurations and the $\mathcal{O}_{\pi\pi(111)}$ operator. In the second column we give the result obtained from the full set of 96 combinations of source/sink momentum; in the third we use parity to reduce this to 48, and in the fourth column we add the axis-permutation symmetry reducing this further to 16 combinations. In the final column we demonstrate the effect, after the global usage of the parity symmetry, of utilizing the three symmetries with *fixed total momentum*, resulting in 21 required momentum combinations.

Table 2 that utilizing the parity symmetry results in no significant increase in the statistical error, but including the axis permutation symmetry increases the error. This suggests that the data associated with the three orthogonal orientations of total $\pi\pi$ momentum; $(\pm 1, 0, 0)\frac{2\pi}{L}$, $(0, \pm 1, 0)\frac{2\pi}{L}$ and $(0, 0, \pm 1)\frac{2\pi}{L}$ are largely uncorrelated and should all be computed to minimize the statistical error. As the combination of parity and the auxiliary diagram symmetry preserves the total momentum, as does swapping the two axes in which the momentum components are zero, we can first apply parity on the total momentum (at no statistical cost) and then further reduce the number of measurements at fixed total momentum; we see from Table 2 that this does not affect the statistical error. We found a similar picture for the other two sets of total momentum: the different orientations (up to parity) are largely uncorrelated, but if we apply the various symmetries at fixed total momentum we do not affect the statistical error.

For our extended measurement programme, utilizing parity reduces the number of required momentum combinations by $2\times$, and a further factor of $4.3\times$ reduction is achieved by applying the symmetries at fixed total momentum. We thus reduce our 7848 contractions to just 1037, a $7.6\times$ total reduction, and the expected calculation time is reduced to a manageable 3.7 hours.

In Table 3 we give the actual time breakdown on 512-nodes of BG/Q. The total of 29 hours is only $\sim 45\%$ larger than our original calculation despite the significant increase in scope thanks to significant optimization effort including a factor of 2.5 improvement in the timing of the $\pi\pi$ two-point function contractions to just 1.5 hours versus the 3.7 hours predicted above. At the time of writing we have completed 339 new measurements primarily with the BG/Q resources at BNL, and recently on the NERSC Cori (Intel KNL) machine.

5. Conclusions

Through analysis of $\pi\pi$ two-point function data with an additional scalar (\mathcal{O}_σ) operator we now have strong evidence of a nearby finite-volume excited state that when taken into account appears to resolve the $\sim 2\sigma$ discrepancy between the value of the $I = 0$ $\pi\pi$ scattering phase shift we published in Ref. [1] and that predicted via dispersion theory coupled with experimental input [5]. In order to ascertain the effect of this excited state upon our calculation of A_0 we have now included the \mathcal{O}_σ operator in the $K \rightarrow \pi\pi$ calculation, as well as adding an additional zero momentum $\pi\pi$ operator with larger individual pion momenta to both the two- and three-point functions. We have also begun computing the $\pi\pi$ two-point functions with non-zero total momentum, which will enable us to obtain the phase shift at a range of additional center of mass energies, providing more

| Description | Time (hours) |
|--|--------------|
| Light quark Lanczos | 5.78 |
| Light quark A2A vectors | 4.48 |
| Heavy quark A2A vectors | 2.68 |
| Gauge fix | 0.31 |
| Kaon meson fields and 2pt function | 0.52 |
| $K \rightarrow \sigma$ contractions | 0.67 |
| Sigma 2pt function | 0.02 |
| Light-light 1s pion meson fields | 5.23 |
| $\pi\pi \rightarrow \sigma$ 2pt function | 0.06 |
| $K \rightarrow \pi\pi$ contractions | 7.02 |
| Pion 2pt function | 0.01 |
| $\pi\pi$ 2pt contractions | 1.51 |
| Configuration total | 29.10 |

Table 3: A breakdown of the job timing on 512-nodes of an IBM BlueGene/Q computer. Here “ $\pi\pi$ ” refers to both the $\mathcal{O}_{\pi\pi(111)}$ and $\mathcal{O}_{\pi\pi(311)}$ operators, and “ σ ” is shorthand for \mathcal{O}_σ .

points that can be compared to dispersion theory as well as allowing a more reliable lattice calculation of the Lellouch-Lüscher finite-volume correction to the $K \rightarrow \pi\pi$ matrix elements. In order to make this extended calculation tractable we have systematically investigated the use of lattice symmetries to reduce the number of combinations of source and sink pion momenta (at fixed total $\pi\pi$ momentum) required to compute the two-point functions, resulting in a $7.6\times$ reduction in the corresponding measurement time with strong evidence that the statistical error remains unchanged. Coupled with extensive code optimizations our resulting measurement time is only 45% larger than before. To date we have generated ~ 340 measurements and have begun preliminary analysis with the aim of publishing an updated result in the next six months.

References

- [1] RBC, UKQCD collaboration, Z. Bai et al., *Standard Model Prediction for Direct CP Violation in $K \rightarrow \pi\pi$ Decay*, *Phys. Rev. Lett.* **115** (2015) 212001 [1505.07863].
- [2] L. Lellouch and M. Luscher, *Weak transition matrix elements from finite volume correlation functions*, *Commun. Math. Phys.* **219** (2001) 31 [hep-lat/0003023].
- [3] G. Buchalla, A. J. Buras and M. E. Lautenbacher, *Weak decays beyond leading logarithms*, *Rev. Mod. Phys.* **68** (1996) 1125 [hep-ph/9512380].
- [4] M. Luscher and U. Wolff, *How to Calculate the Elastic Scattering Matrix in Two-dimensional Quantum Field Theories by Numerical Simulation*, *Nucl. Phys.* **B339** (1990) 222.
- [5] G. Colangelo, J. Gasser and H. Leutwyler, *$\pi\pi$ scattering*, *Nucl. Phys.* **B603** (2001) 125 [hep-ph/0103088].
- [6] T. Wang and C. Kelly, *Studies of $I=0$ and 2 π - π scattering at kaon mass with physical pion mass in GPBC*, *PoS LATTICE2018* (2018) 276.
- [7] C. Kelly, *Progress in the improved lattice calculation of direct CP-violation in the Standard Model*, *EPJ Web Conf.* **175** (2018) 13020.
- [8] J. Foley, K. Jimmy Juge, A. O’Cais, M. Peardon, S. M. Ryan and J.-I. Skullerud, *Practical all-to-all propagators for lattice QCD*, *Comput. Phys. Commun.* **172** (2005) 145 [hep-lat/0505023].